628: EXPERIMENTAL INVESTIGATION OF FLUID FLOW REGIME IN THERMOSYPHON HEAT-PIPE EVACUATED TUBE SOLAR WATER HEATERS

David A G Redpath [1]*, Philip W Griffiths [2], Steve N G Lo[3], Madonna Heron[4],

Centre for Sustainable Technologies, University of Ulster, Newtownabbey, Northern Ireland [1]*
d.redpath@ulster.ac.uk
Centre for Sustainable Technologies, University of Ulster, Newtownabbey, Northern Ireland [2]
Centre for Sustainable Technologies, University of Ulster, Newtownabbey, Northern Ireland [3]
School of Computing and Mathematics, University of Ulster, Newtownabbey, Northern Ireland [4]

Abstract

Previous studies have reported that the adoption of thermosyphon fluid circulation can reduce the capital cost of solar water heating systems. Well designed thermosyphon systems are as effective as pumped systems but with lower capital and running costs. To investigate this; two experiments were undertaken. Firstly a thermosyphon heat-pipe Evacuated Tube Solar Water Heater (ETSWH) was assembled using a proprietary collector and its performance monitored under a northern maritime climate. Secondly a transparent physical model was fabricated to the same dimensions as the proprietary collector's manifold and the internal fluid flow regime was observed using particle imaging velocimetry. The annual monitored performance of the thermosyphon heat-pipe ETSWH demonstrated that this system could supply a solar fraction of 0.4, 0.45 and 0.71 towards the average hot water load of a detached, semi detached and terraced dwelling respectively.

Keywords: Thermosyphons, evacuated, heat-pipe

1. Introduction

The current cost of installed solar water heating systems in the United Kingdom range from £3200-£4500, [1]. The annual efficiency of well designed Flat Plate Solar Water heaters, (FPSWHs) and Evacuated Tube Solar Water Heaters, (ETSWHs) has been reported as 35-40% and 45-50% respectively [2]. In Northern maritime climates, ETSWHs utilising heat-pipe absorbers are particularly appropriate. This is due to the unique thermal properties of heat-pipes, i.e. freeze resistance, self regulating heat transfer, the ability to transport heat against gravitational forces and the ability to act as a thermal diode, reducing heat loss from the absorber. Unfortunately heat-pipe ETSWHs have a high capital cost reducing their attractiveness to consumers. Two methods for reducing the costs of heat-pipe ETSWHs are proposed and considered in this study; the adoption of thermosyphon fluid circulation and the incorporation of reflective concentrators. Previous studies have reported that well designed thermosyphon solar water heating systems are as effective as pumped systems but with lower capital and running costs, [3]. Thermosyphon ETSWHs do not require parasitic energy or an associated control unit; to transfer the collected solar energy to a hot water storage tank. Current costs of pumped controlled units range from £200 to £400. Thus adoption of thermosyphon fluid circulation would reduce the installed costs by 4% to 12.5%. The absence of moving parts suggests that reliability would be increased if passive control mechanisms such as thermosyphon fluid circulation were utilised. The shorter flow path within heat-pipe ETSWHs implies a lower frictional resistance to fluid flow than equivalent sized direct flow ETSWHs. Globally over 90% of installed domestic solar water heaters utilise thermosyphon fluid circulation to transfer solar gain from the solar collector to the hot water storage tank, [4]. Yet in the United Kingdom thermosyphon fluid circulation is rarely utilised for solar water heating systems. The two barriers to increasing the uptake of these systems is that retro fitting to existing properties would be difficult as the hot water tank must be located above the collector. Secondly no specific information is available for planners, architects or installers regarding the thermal performance of thermosyphon solar water heating systems in Northern maritime climates. Recent research on evacuated solar thermal systems has considered only direct flow ETSWHS subjected to climatic conditions very different from Northern maritime regions. The thermal performance of a commercial close-coupled thermosyphon glass concentric counter flow ETSWH was evaluated using an internationally recognised test procedure, [5]. Under the load conditions specified in the Australian solar water heating standards, this system achieved a 55% reduction in energy usage, when supplying thermal energy to preheat a domestic hot water supply, [6]. A similar study, [7], evaluated another commercial close-coupled thermosyphon glass concentric counter flow ETSWH again using the same internationally recognised procedure. The experimental data was used to develop a numerical model of the collector which predicted thermal performance for this system as a solar pre-heater delivering nocturnal hot water loads for locations in Australia, China and Europe, to an accuracy of ±5% [5]. Figure 1 depicts a schematic diagram of a distributed thermosyphon heat-pipe ETSWH.

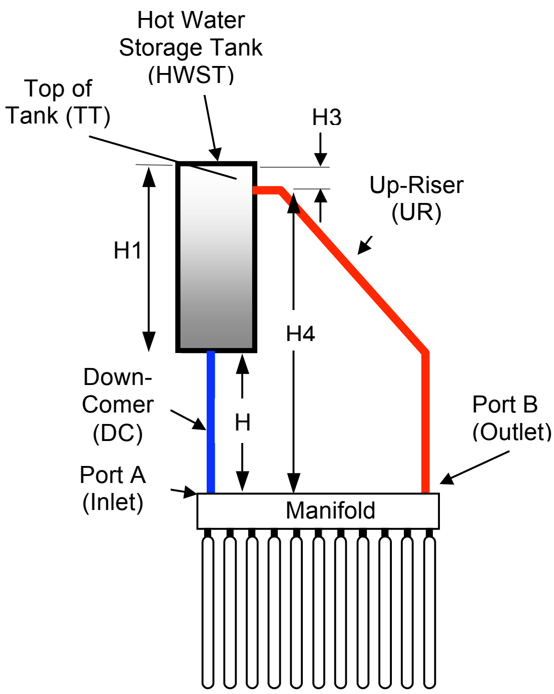

Fig. 1 Schematic thermosyphon heat-pipe ETSWH

Existing knowledge of thermosyphon circulation within the manifold chamber of heat-pipe ETSWHs is limited; the most similar situation to this is that of an interactive pin-fin array. This represents an interesting heat transfer problem as each upstream pin-fin (condenser) influences downstream pin-fins through either an increase in the localised fluid temperature or by the generation of buoyant flow. The first effect reduces heat transfer on downstream fins whereas the second increases it. Thus the spacing of the pin-fins is critical if optimal performance is to be realised. If reflective concentrators are to be incorporated the surface heat flux of the condensers will be increased, changing the internal fluid flow regime. Thus knowledge of heat transfer under these conditions is required if these designs are to be optimised. The thermal performance and cost effectiveness of evacuated systems is improved through the integration of concentrators as the amount of solar radiation collected per unit area of absorber is increased, thus reducing the number of evacuated tubes required. The adoption of a reflective concentrator decreases radiative heat loss as the area of radiating surface is reduced relative to total collector area, [8]. Previous related studies [9, 10, 11, 12, 13, and 14] have only considered idealised situations with regular but simple cavity geometries. The manifold chamber of a proprietary heat-pipe ETSWH differs from the idealised situations considered in all previous research by having an irregular six sided cross section. An experimental investigation undertaken at the University of Ulster concerned with thermosyphon fluid circulation under Northern maritime climates identified that a thermosyphon heat-pipe ETSWH was prone to diurnal reverse fluid flows. This reduced the efficiency of solar storage by 13% as the reversed fluid flow degraded thermal stratification within the hot water storage tank via convective entrainment and increased fluid mixing [15]. A further study [16] found that the occurrence of diurnal reverse fluid circulation was reduced from 69% to 22% by increasing the horizontal inclination of the collector manifold from 1° to 5°. The average diurnal efficiency of a thermosyphon heat-pipe ETSWH over 6 months was found to be 64.7%. Payback periods for this experimental system were 9.6 to 26.1 years and 3.4 to 7.9 years for scenarios of no grant aid and with grant aid respectively. This compared favourably with the payback period of a typical forced circulation solar water heating system.

Firstly this paper presents further information from the same system which is currently installed at the University of Ulster. Secondly a physical laboratory model of the manifold chamber was fabricated to investigate the internal thermosyphon fluid flow regime. This data will be of use to designers and architects as well as heat transfer studies. It is hoped that this data will stimulate interest in the application of thermosyphon fluid circulation for reducing the cost of solar thermal systems under Northern maritime climates.

2. Methodology

A previous study on the long-term performance of thermosyphon solar water heaters reported that a minimum test period of at least 6 months is required to obtain the necessary data required to produce a design tool for prediction of system performance, [17].

Two experiments were undertaken: Firstly a proprietary heat-pipe evacuated tube solar collector was assembled, incorporated within a system and subjected to the Northern maritime climatic conditions of the outdoor test facility at the University of Ulster for one year. Incident solar radiation was measured to an accuracy of ±3%, temperature measurements were made at the collector inlet (port A), collector outlet (port B), Hot Water Storage Tank (HWST) inlet; HWST outlet and the ambient using class A platinum resistance thermometers (accuracy±0.06°C). Temperatures inside the HWST were measured using a vertical array of thermocouples located along the central axis of the HWST (accuracy ±0.1°C). The accuracy of the sensors used was confirmed via laboratory calibration. When immersed in an isothermal medium the standard deviation between the class A platinum resistance thermometers and the T-type thermocouples was 0.06 and 0.1 respectively. All measurements were sampled every 10 seconds, averaged over a five minute period and then recorded using a multi-channel logger. A simple evening peak load pattern was applied to this system.

Secondly a physical model of the manifold chamber of the evacuated tube solar collector in question was fabricated from Polyethylene Terephthalate Polyester (PET) by using a thin heated wire to bend it to the same geometry and dimensions as the proprietary collector manifold chamber. Figure 2 depicts the external dimensions of the PET model manifold. (In the proprietary ETSWH selected for this study, the pin-fin pitch to diameter ratio was 3.2, and the array of non-isothermal condensers is typically inclined to within ±10° to the latitude of location to ensure optimal solar energy collection.

A previous study found that a 10 pin-fin model manifold operated under steady laboratory conditions accurately simulated the output of 1m^2 of a thermosyphon heat-pipe ETSWH, [16].

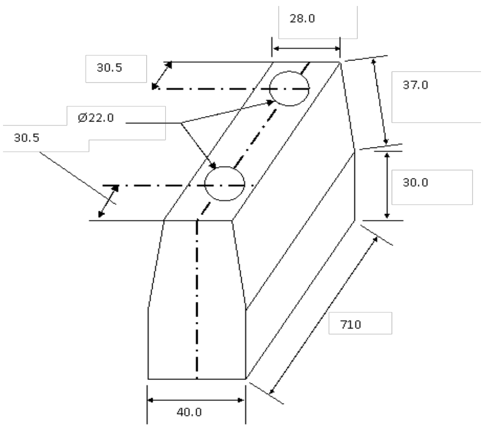

Fig. 2 Three dimensional cross section depicting external dimensions of a model manifold chamber (mm)

The condenser array was physically simulated using solid copper cylinders (pin-fins) with an electric element inserted. These were wired in series allowing the power supplied to be carefully controlled and maintained. The design of this model manifold allowed the heating elements to be replaced and pin-fins to be removed. This meant that the removal of evacuated tubes and higher heat fluxes on the condensers could be simulated under steady conditions to investigate the effects of increased condenser spacings and fluxes. Under steady state conditions the rate of heat transfer (Q) from each pin-fin/condenser to the surrounding fluid would be constant so flux conditions were assumed to be similar. Figure 3 shows the internal dimensions of the PET model manifold. Two different pin-fin arrangements were investigated using the PET model manifold and both of these were under simulated conditions of 1000Wm^{-2}; firstly 10 pin-fins were used, then every pin-fin was removed and the 100W cartridge heaters in the remaining five pin-fins were replaced by five 200W cartridge heaters. This had the effect of keeping the thermal input the same but halving the area available for heat transfer.

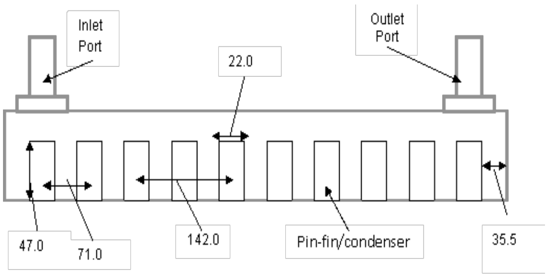

Fig. 3 Side view of internal dimensions (mm) model manifold chambers

The purpose of this was to simulate the removal of half the evacuated tubes and the incorporation of reflective concentrators. Two Dimensional Particle Imaging Velocimetry (2D-PIV) was then used to visualise the fluid flow regime in the PET manifold. The liquid was seeded with buoyantly neutral particles and then illuminated with a class 4 Yttrium Aluminium Garnet (YAG) laser. Image pairs were taken with a camera synchronised to the laser. Image processing software enabled tracking of particles through the flow field, allowing the magnitude and direction of the thermosyphon fluid flow to be quantified. Fifty double frame images of the fluid flow field around the manifold inlet, middle section and manifold outlet were captured; the frequency of the laser pulses was set at 10 Hz with a camera exposure time of 10,000μs.

3. Results

3.1 Thermosyphon heat-pipe ETSWH

The thermal performance of the thermosyphon heat-pipe ETSWH was monitored from 1st February 2007 to January 2008, providing a year of experimental data. The storage of incident solar radiation (Q_{stored}) was calculated by measuring the diurnal change in the temperature of the hot water storage tank (ΔMBTT) using equation 1.

$$Q_{stored} = (\Delta MBTT) * C_p * m \quad [1]$$

The diurnal efficiency of the thermosyphon heat-pipe ETSWH was calculated using equation 2.

$$\eta = \frac{Q_{stored}}{G_T * A_c} \quad [2]$$

The mean energy content of incident solar radiation on the collector plane and average diurnal efficiency were calculated as 2.89kWh/m^2/day and 63.7% respectively. The total energy collected by this system over one year was measured as 1338kWh. In the UK there are three generic building types: detached, semi detached and terraced [18], with reported annual heating hot water requirements of 3054kWh, 3500kWh and 1947kWh respectively. The solar fraction of the heating load that this system could supply for each type of domicile was calculated then using equation 3.

$$f = \frac{\text{Supplied Solar Energy (kWh)}}{\text{Hot Water load (kWh)}} \quad [3]$$

Figure 4 shows the solar fraction of the hot water load that could be met by the thermosyphon heat-pipe ETSWH for each UK building type.

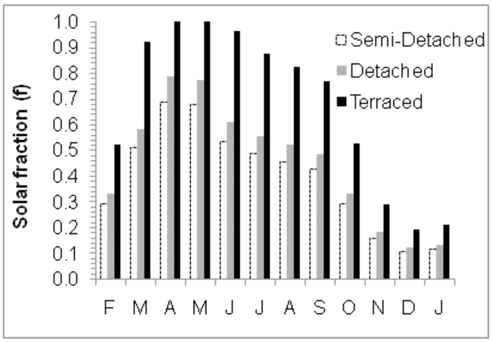

Figure 4 Solar fraction of heating load for different UK domicile types

3.2 PET Model Manifold

The internal heat transfer regime was then examined using the results from the PET model manifold. The total energy stored using 10 pin-fins and 5 pin-fins were calculated using equation 1 as 353W and 312W respectively. So under similar conditions the efficiency of using 5 pin-fins was only 4% less than that when using 10 pin-fins. To examine interactions between the pin-fins in the array the temperatures of the pin-fins were normalised with respect to the temperature difference between free stream conditions and the surface temperature of the lowermost pin-fin in the array. Normalised temperatures were calculated using equation 4 [9] where T_s was the surface temperature of the pin-fin in question, T_∞ represented free stream conditions and T_{spf1} was the surface temperature of the lowermost pin-fin in the array.

$$\theta = \frac{(T_s - T_\infty)}{(T_{spf1} - T_\infty)} \quad [4]$$

These were plotted against X/X_{max} where X is the distance of the pin-fin in question from the lowermost pin-fin and X_{max} is the distance between the top and bottom pin-fin in the array as shown in figure 5. The maximum error in calculating the normalised temperatures was ±0.37%.

The Nusselt number (Nu_x) for each pin-fin was calculated using equation 5, [19]; where h was the convective heat transfer coefficient, k was the thermal conductivity of the fluid and δ was the characteristic length. The characteristic length (δ) used for pin-fins 2 to 10 was the distance from the lowermost pin-fin [9]. The characteristic length (δ) used for the lowermost pin-fin (pin-fin 1), was for a single smooth inclined cylinder experiencing natural convection [10]. The Nusselt number for pin-fin 1 was calculated using the characteristic length proposed by [10] for natural convective heat transfer from an inclined smooth cylinder. All fluid properties were evaluated at the film temperature.

$$Nu = \frac{h\delta}{k} \quad [5]$$

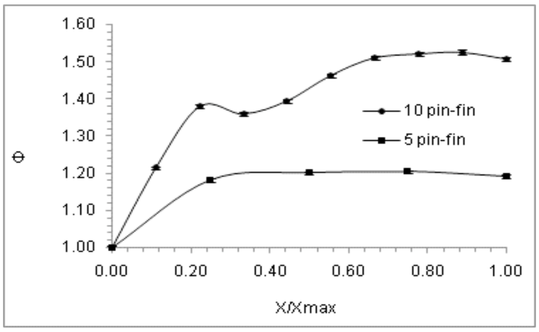

Fig. 5 Normalised Temperatures along the pin-fin array in the PET model manifold experiment

The Rayleigh number (Ra_x) was calculated using equation 6 [19]. Where g was the acceleration due to gravity, β the coefficient of cubical expansion, v represented kinematic viscosity, δ the characteristic length and Pr the Prandtl number.

$$Ra = \frac{g\beta(T_s - T_\infty)\delta^3}{\nu^2} Pr \quad [6]$$

The Nusselt numbers calculated for each of the pin-fins in the 10 pin-fin and five pin-fin experiments were then normalised with respect to the expected Nusselt number calculated for an individual pin-fin (Nu_i) undergoing natural convective heat transfer using equation 7 [10]. The results are shown in figure 6 the error in calculating the Nusselt number was ±3.8%. Figure 7 shows the relationship between the Rayleigh number and Nusselt number.

$$Nu_i = 0.125 Ra^{0.333} \quad [7]$$

PIV images from the PET manifold simulation were then collected to see whether the differences in heat transfer shown in figures 5 and 6 could be visualised. Image processing was required to remove outlying and erroneous vectors, details of the image processing software and the adaptive correlations used are discussed in [20]. Figure 8 depicts the stream lines measured around pin-fins 2 and 3 when the manifold had 10 fins. Figure 9 depicts the stream lines from the same region using 5 fins in the manifold. Figures 10 and 11 depict the uppermost regions that could be observed using the experimental apparatus for the 10 pin-fin and 5 pin-fin experiments respectively.

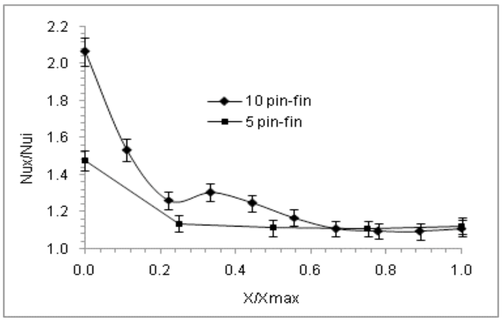

Fig. 6 Normalised Nusselt numbers in PET manifold

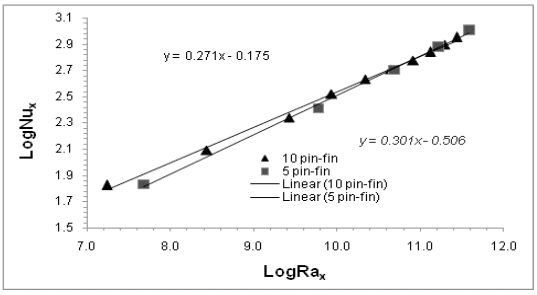

Fig.7 Rayleigh and Nusselt numbers

Direction of fluid flow, mean velocity =0.004ms^{-1}

Figure 8 Stream lines 10 fins around pin-fin 2 and 3

Direction of fluid flow, mean velocity =0.010ms^{-1}

Figure 9 Stream lines 5 fins around pin-fin 1

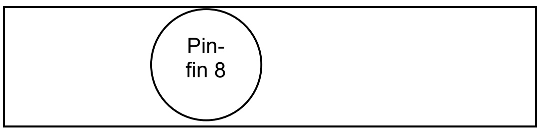

Direction of fluid flow, mean velocity =0.004ms^{-1}

Fig. 10 Ten pin-fin experiment stream lines around pin-fin 8

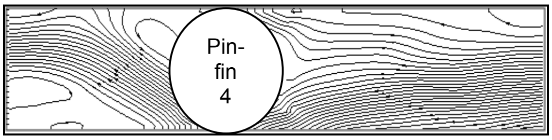

Direction of fluid flow, mean velocity =0.007ms^{-1}

Fig. 11 5 pin-fin experiment stream lines around pin-fin 4

4. Analysis of Results

The results gathered from monitoring a thermosyphon heat-pipe ETSWH have demonstrated that such systems compare favourably in comparison to the figures quoted in section 1 for typical forced circulation systems. Using the 2007 metrological data collected from the test location the described system supplied an annual solar fraction equivalent to 0.4, 0.45 and 0.71 for semi-detached, detached and terraced dwellings respectively. When 10 pin-fins were used it was observed that sufficient flow was generated which reduced the normalised temperature relative to the preceding pin-fin in the array at pin-fins 4 and 10. This was mirrored by a rise in the normalised Nusselt number. When the pitch was doubled and only 5 pin-fins were used a different situation arose. From figure 5 and 6 it was observed that normalised temperatures for pin-fins 3 and 4 were the same and a small decrease occurred at pin-fin 5. The characteristics of the fluid flow regime were more laminar when only 5 pin-fins were used. As evidenced by the stream lines shown in figures 7 to 10, when the array was comprised of 10 pin-fins the fluid flow regime was more turbulent and velocity reduced. Much greater frictional losses occurred when the 10 pin-fins array was used. Whilst the 5 pin-fin array had only half the surface area of the 10 pin-fin array, the efficiency was only 4% less when the same thermal input was supplied.

5. Conclusion

An experimental thermosyphon heat-pipe ETSWH exposed to a Northern maritime climate and monitored for one year has been shown to have an annual diurnal efficiency of 63%. This figure compared favourably to performance figures quoted in the literature. Further work required in this area is an investigation of incorporation of non-imaging CPC's and the effect on the fluid flow regime within the manifold for an east-west orientation as this will mean that the pin-fin array will be vertical. Different hot water load patterns should be applied to the system to produce a validated design tool.

6. Acknowledgements

The authors would like to thank the technical staff involved, specifically Paul Annesley, Jim Bailie Alan Carnduff, Philip Dalzell and Jim Dickson. David Redpath would like to thank the contribution of Professor Phil Eames towards this work during his doctoral studies.

7. References

1. Energy Saving Trust, [Online], Available:www.energysavingtrust.org.uk[14th June 2008]
2. DGS, (2005). Planning and installing solar thermal systems: a guide for installers, architects, the German Solar energy society, James and James, London, UK
3. Norton B., Eames P. C. and Lo S. N. G., (2001). Alternative approaches to thermosyphon solar energy water heater performance analysis and chararacterisation, *Renewable and sustainable energy reviews*, 5: p.79-96
4. Garcia-Valladares O., Pilatowsky I., Ruiz V., (2008). Outdoor test method to determine the thermal behaviour of solar domestic water heating systems. *Solar Energy, Article in Press (ISES)*, Perth, Australia.
5. Anon, (1995). Solar heating-Domestic water heating systems, Part2: Outdoor test methods for system performance characterization and yearly performance prediction solar-only systems, *ISO 9459-2, International Standard*
6. Budihardjo I., Morrison G. and Behnia M., (2002). Performance of a water-in-glass evacuated solar water heater, *Proceedings of Australian New Zealand Solar Energy Society*, Newcastle, Australia
7. Morrison G. L., Budihardjo I., Behnia M., (2004). Water-in-glass evacuated tube solar water heaters, *Solar Energy*, 76(1-3): p.135-140
8. Garrison J. D., (1979), Optimisation of fixed solar thermal collectors, *Solar Energy*, 23(2): p.93-102
9. Marsters G. F., (1972). Arrays of heated horizontal cylinders in natural convection, *International Journal of Heat and Mass Transfer*, 15(5): p.921-933
10. Morgan V. T., (1975). The Overall Convective heat transfer from smooth circular cylinders, *Advances in heat transfer*, 11: p.199-264
11. Farouk B. and Guceri S. I., (1983). Natural convection from horizontal cylinders in interacting flow fields, *International Journal of Heat and Mass Transfer,* 26(2): p.231-243
12. Corcione M., (2005). Correlating equations for free convection heat transfer from horizontal isothermal cylinders set in a vertical array, International *Journal of Heat and Mass Transfer*, 48(17): p. 3660-3673
13. Morrison G. L., Budihardjo I., Behnia M., (2005). Measurement and Simulation of Flow Rate in a Water-in-glass evacuated tube solar water heater, *Solar Energy*, 78(2): p.257-267
14. Corcione M., (2007). Interactive free convection from a pair of vertical tube-arrays at moderate Rayleigh numbers, *International Journal of Heat and Mass Transfer*, 50(5-6): p. 1061-1074
15. Redpath D. A. G., Lo S. N. G. and Eames P. C., (2007), Diurnal reverse fluid flow in thermosyphon evacuated tube solar water heaters in a Northern Maritime Climate, *Proceedings of Heat Set Conference*, Chambery, France, 18th-20th April
16. Redpath D. A. G. (2007). An experimental investigation of thermosyphon heat-pipe evacuated tube solar water heaters subjected to a Northern Maritime Climate, PhD Thesis, University of Ulster, Northern Ireland, UK
17. Morrison G. and Sapsford C., (1983). Long term performance of thermosyphon solar water heaters, *Solar Energy*, 30(4): p.341-350
18. Singh H., Eames P. C. and Peacock A., (2007). Reducing the carbon footprint of existing UK dwellings-case studies, *Proceedings Heat-set*, Chambery, France, 18th-20th April
19. Incropera F. P. and DeWitt D. P., (2002). Introduction to heat transfer, *John Wiley and sons*, 4th edition, New York, USA
20. Anon, (2002).Flow manger software and introduction to PIV instrumentation, *Dantec dynamics, 5th edition*, Tonsbakken, Denmark

8. Nomenclature

A_c-Area of Collector (m^2)
C_p-specific heat capacity (Jkg^{-1})
f -Solar fraction
g- Acceleration due to gravity (ms^{-2})
h- Convective heat transfer coefficient ($W/m^{-2}K^{-1}$)
k- Thermal conductivity ($Wm^{1}K^{-1}$)
m-mass (kg)
Nu-Nusselt number
Pr- Prandtl number
Q- Energy transfer rate (W)
Ra-Rayleigh number
T-Temperature (°C)
X-distance (m)

8.1 Greek Nomenclature

Β- Coefficient of cubical expansion (K^{-1})
Φ- Normalised temperature
Δ-Temperature difference (°C)
η-Efficiency
δ-Characteristic length (m)
ν-kinematic viscosity ($m^2.s^{-1}$)

8.2 Abbreviations

ETSWH- Evacuated tube solar water heater
FPSWH- Flat plate solar water heater
HWST- Hot water storage tank

8.3 Subscripts

f-Final
i-Initial, individual
max-maximum
s-surface
spf1-surface pin-fin 1
x-length based
∞-free stream conditions